

## ANISOTROPY OPTIMIZATION OF GIANT MAGNETOIMPEDANCE SENSORS

P. Ciureanu\*, G. Rudkowska, L. Clime, A. Sklyuyev, A. Yelon

École Polytechnique Montréal, Département de génie physique and  
Regroupement québécois sur les matériaux de pointe (RQMP), CP 6079,  
succursale Centre-ville, Montréal, Québec, H3C 3A7, Canada

As-cast melt extracted CoFeSiBNb wires 37.5  $\mu\text{m}$  in average diameter prepared by MXT Inc. of Montréal have a predominantly helical anisotropy due to residual tensile and torsional stresses quenched in during preparation. When a supplementary tensile stress is applied along the wire, its easy axis of magnetization rotates towards the transverse (or circumferential) direction, since the magnetostriction of Co-rich wires is negative. Well defined, high amplitude and steep peaks of the magnetoimpedance are obtained when the magnetoelastic anisotropy of the wire reaches an optimum in magnitude and orientation. This optimum may be obtained by fine tuning the applied stress and can be permanently quenched in the material by current annealing the wire. A 50 to 100 mA DC current was used for this purpose. The circumferential DC magnetic field associated with this current also changes the wire anisotropy. After cooling, the wire quenches-in an optimum anisotropy, which maximizes the GMI effect of the wire. Magnetic field sensors with sensitivities as high as 1 kV/(T mm) and figures of merit of about 16  $\Omega\text{T}$  were obtained as a result of this optimization, for wires driven by AC currents of 1 mA<sub>rms</sub> amplitude and 10 MHz frequency.

(Received April 14, 2004; accepted June 22, 2004)

*Keywords:* Magnetic field sensors, Giant magnetoimpedance effect, Magnetoelastic anisotropy

### 1. Introduction

Rapid solidification of amorphous wires generates strong tensile and torsional stresses, which are quenched in the material and contribute to the effective anisotropy of the wire. These wires are characterized by a core-shell magnetic structure [1]. The spins in the inner core are oriented along the axial direction, while those in the outer shell are radial or circumferential, depending on the wire magnetostriction. In the case of a wire with negative magnetostriction, the magnetoelastic coupling of the residual stresses with the spins in the shell tends to orient them in a direction which is helical with respect to the wire length [2]. When tensile stress is applied [3], the transverse anisotropy is reinforced, that is, these spins rotate toward the circumferential direction. In these situations, the radius of the inner core tends to shrink, since its spins turn away from the axial direction. Optimization of the circumferential magnetoelastic anisotropy can be achieved by applying a tensile stress to the wire, by current annealing of the same wire or by applying a DC current which biases the AC current carried by the wire.

CoFeSiBNb amorphous wires prepared by melt-extraction by MXT, Inc. of Montreal were used in this study. These wires had an average radius of 17.5  $\mu\text{m}$  and were 4, 8 or 12 cm long. If such wires carry AC currents whose frequency is higher than 1.5 MHz, the skin effect in the magnetic conductor causes the current to flow near the wire surface. (The skin depth,  $\delta = \sqrt{2\rho / f\mu_\phi}$ , where  $\rho$  is the wire resistivity,  $f$  the frequency and  $\mu_\phi$  the circumferential magnetic permeability,

---

\*Corresponding author: petru.ciureanu@polymtl.ca

equals the wire average radius at about 1.5 MHz.) For a constant resistivity, the skin depth shrinks when the frequency and the magnetic permeability increase. This causes the resistive part of the wire impedance to increase. Moreover, the AC current produces a circumferential magnetic field,  $h_\phi$ , which magnetizes the wire. Thus, the reactive part of the wire impedance changes with frequency and magnetic field, due to the variation of the intrinsic wire inductance  $L = \mu_\phi \lambda / 2\pi$  [4], where  $l$  is the wire length. Tensile stress also changes this impedance through changes in the induced magnetoelastic anisotropy of the wire. Thus, the giant magnetoimpedance (GMI) response of the wire represents the variation of the impedance of a magnetic conductor carrying an AC current of frequency  $f$ , submitted to a tensile stress,  $\sigma$ , as a function of an applied DC field,  $H$ :  $Z(f, \sigma, H)$ .

Well defined, high amplitude and steep peaks of the GMI response are obtained when the circumferential anisotropy of the wire reaches an optimum in magnitude and orientation. This optimum may be obtained by fine tuning the applied stress and can be permanently quenched in the material by current annealing the wire. The goals of this paper are to describe the means of reaching the optimum circumferential anisotropy which maximizes the GMI effect and those of quenching it into the wire.

## 2. Experiment

$\text{Co}_{80.89}\text{Fe}_{4.38}\text{Si}_{8.69}\text{B}_{1.52}\text{Nb}_{4.52}$  (wt%) wires have a resistivity of  $130 \mu\Omega \text{ cm}$  and a saturation magnetization of  $660 \text{ kA/m}$  ( $\text{emu/cm}^3$ ). Their circumferential relative magnetic permeability measured in zero axial field at 10 MHz is 632 [5]. Their diameter was measured using a red laser and ranged from  $31.5$  to  $38.6 \mu\text{m}$ . Axial DC magnetic fields up to  $300 \text{ Oe}$  were applied to the wire using a pair of Helmholtz coils. Tensile stresses up to  $500 \text{ MPa}$  were applied to the wire using a mechanism driven by a micrometre gauge. A DC annealing current up to  $100 \text{ mA}$  was applied to the wire under stress using a constant current source. Giant Magnetoimpedance (GMI) responses of these wires were measured as functions of the axial DC field,  $H$ , for given frequency and tensile stress. These were plotted using an impedance analyzer which provided the wire with an AC current of variable amplitude (up to  $10 \text{ mA}_{\text{rms}}$  effective current) and frequency (up to  $13 \text{ MHz}$ ) and measured the real and imaginary parts of the wire impedance at each set of values of frequency, axial field and stress. All the GMI responses shown here are for a  $10 \text{ MHz}$  driving current with an amplitude of  $1 \text{ mA}_{\text{rms}}$ . The wire under test was always demagnetized before the measurement.

The circumferential hysteresis loop of the wire was plotted using a conventional Wheatstone bridge, with the wire mounted as an arm. The current density passing through the wire was about  $7.5 \text{ A/m}^2$ , much less than that usually employed for self-annealing amorphous materials ( $40 \text{ A/m}^2$ ) [6, 7], so that the wire properties remained unchanged. The amplitude of the drive field at the surface of the wire,  $h_\phi$ , was  $0.84 \text{ Oe}$ , sufficient to produce a major hysteresis loop in the soft magnetic material. The circumferential hysteresis loop was obtained by time integrating the differential signal picked-up across the bridge, that is a succession of alternating polarity pulses with a frequency of  $10 \text{ kHz}$ . The longitudinal magnetization loop of the wire was plotted with the help of a conventional inductive method using a drive coil wound around the wire and carrying a  $10 \text{ kHz}$  current of  $50 \text{ mA}$  amplitude. The amplitude of the drive field,  $h_z$ , was  $5 \text{ Oe}$ , sufficient to produce a major hysteresis loop in the soft magnetic material. Two pick-up coils, wound in opposition and connected in series, provided a differential signal, consisting of a succession of alternating polarity pulses with a frequency of  $10 \text{ kHz}$ . The longitudinal hysteresis loop was obtained by time integrating this signal.

## 3. Optimization of the circumferential magnetoelastic anisotropy of the wire

When the frequency of the AC current carried by the wire changes, the real and imaginary parts of its impedance change accordingly. The magnitude of the GMI response increases with frequency. In addition, the magnetic permeability changes non-linearly with frequency, stress and DC magnetic field. Thus, the shape of the MI response changes as well. For a frequency lower than  $1.5 \text{ MHz}$ , the response of an as-cast wire shows two equal-amplitude peaks located on the field axis

at values close to the circumferential anisotropy field of the wire,  $H_{\text{peak}} = \pm H_K$ . This response is symmetrical and slightly hysteretic at low fields, showing that irreversible changes occur in the magnetic structure. If the frequency of the current is increased to 10 MHz, these peaks are located at fields larger than  $H_K$ . The DC longitudinal magnetization process in the inner core is domain wall displacement, which leads to Barkhausen jumps of the axial spins occurring at low field. These jumps are also visible in the GMI responses due to the core-shell coupling [8]. In contrast, the magnetization process occurs by rotation in the outer shell of as-cast wires, where circumferential spins rotate towards the direction of the DC longitudinal field.

When tensile stress is applied to the wire, the peaks of the GMI response are still symmetrical but enlarged and more widely spaced on the field axis (Fig. 1).  $H_{\text{peak}}$  increases with tensile stress due to the magnetoelastic field which adds to the circumferential anisotropy field of the wire. At 10 MHz, the peak field of as-cast wires is between  $\pm 0.2$  and  $0.4$  Oe. It increases up to  $\pm 1$  Oe for a tensile stress of 100 MPa and  $\pm 1.7$  Oe for a stress of about 200 MPa. Since the melt-extracted wires have a cross section of about  $1,000 \mu\text{m}^2$ , a 100 MPa tensile stress is the equivalent of 10 grams suspended at one end of the wire. Fig. 2 shows that the peak field depends linearly on tensile stress at both 1 and 10 MHz. The magnetostriction constant of the material, obtained from the slope  $dH_{\text{peak}}/d\sigma \approx H_K/\sigma$  in Fig. 2, is negative and small ( $-1.2 \cdot 10^{-7}$ ). Moreover, the  $H_{\text{peak}}$  vs  $\sigma$  line intersects the stress axis at  $-20$  MPa at 1 MHz and  $-70$  MPa at 10 MHz. This is due to the increase in peak field with frequency predicted by the classical ferromagnetic resonance theory for any tensile stress applied to the wire.

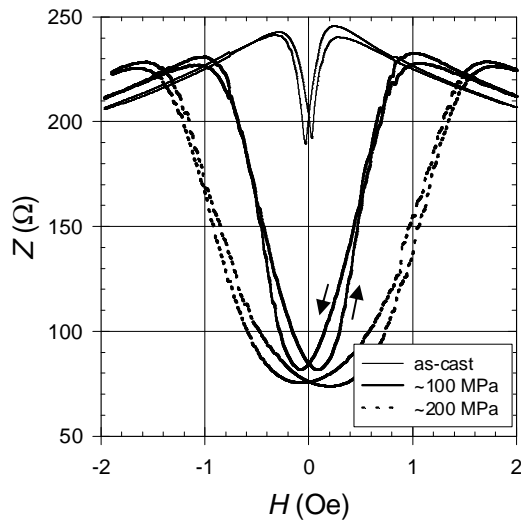


Fig. 1. Giant Magnetoimpedance (GMI) responses of a 4 cm long melt extracted wire. A 10 MHz sensing current with an amplitude of  $1 \text{ mA}_{\text{rms}}$  has been used in this experiment. The arrows show the loading (up) and the unloading (down) responses.

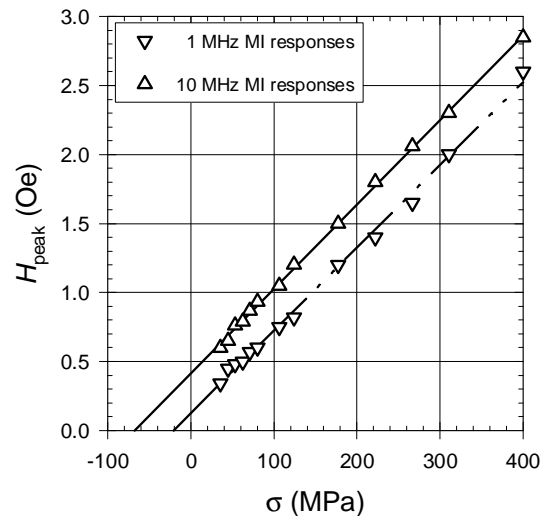


Fig. 2. Peak field of 4 cm long melt-extracted wires vs. tensile stress. 1 and 10 MHz sensing currents with an amplitude of  $1 \text{ mA}_{\text{rms}}$  were used in the experiments.

The circumferential loops of melt extracted wires are shown in Fig. 3. We see that the loop of as-cast wires is shifted with respect to the origin of the driving field,  $h_\phi = 0$  (asymmetry in coercivity). Modeling has shown [9,10] that this asymmetry depends upon the angle formed by the spins in the outer shell of the wire and the transverse axis. This angle increases with torsional stress and decreases with tensile stress. Since no torsion was applied to the wire, this asymmetry must be produced by a residual torsional stress quenched in the wire during melt extraction.

The asymmetry in coercivity of the circumferential loops disappears when a tensile stress of about 40 MPa is applied to the wire (Fig. 3), indicating that this tension compensates the quenched-in torsion. Steeper circumferential loops with larger coercivities were obtained when stress or frequency increased. Fig. 3 also shows that the circumferential loops change from "hard-axis" to "easy-axis"-type when the tensile stress increases from zero (as-cast wires) to 120 MPa. This indicates that, in the absence of an axial static field, the spins in the outer shell of the wire rotate toward the transverse (circumferential) direction. This confirms that the magnetostriction of the melt extracted wire is negative, as expected.

The longitudinal loops of as-cast wires are symmetrical with respect to the origin of its driving field,  $h_z = 0$  for any tensile stress (Fig. 4). Their coercivity decreases while the saturation field increases with tensile stress. This stress turns the spins away from the longitudinal direction, causing the longitudinal permeability of the wire to decrease. Fig. 4 shows that the longitudinal loops change from "easy-axis" to "hard-axis"-type when the tensile stress increases from zero (as-cast wires) to 120 MPa. This confirms again that the spins in the outer shell rotate toward the transverse (circumferential) direction and that the wire magnetostriction is negative.

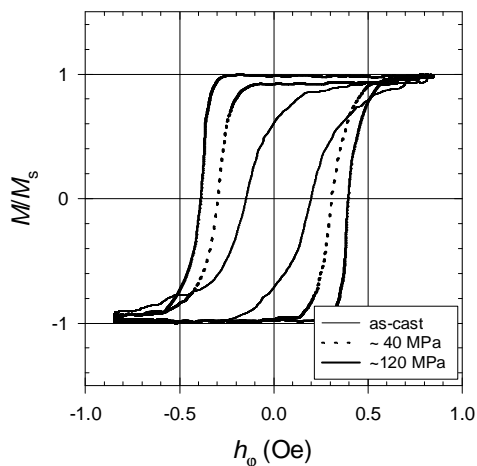


Fig. 3. Circumferential hysteresis loops of 4 cm long melt extracted wires. The 10 kHz driving field had an amplitude of 0.84 Oe at the wire surface.

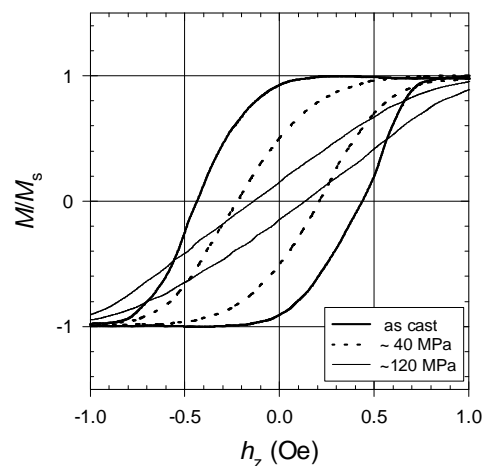


Fig. 4. Longitudinal hysteresis loops of 4 cm long melt extracted wires. The 10 kHz driving field had an amplitude of 5 Oe.

#### 4. Quenching in the wire the optimum anisotropy

We have used a "self-annealing" technique, consisting of passing a DC current through the wire, heating the material. The current-temperature characteristic of the wire was determined by measuring the strength of the DC current which heats the wire to the Curie temperature ( $295^{\circ}$  C for the CoFeSiB alloy, as determined using a furnace [6]). The circumferential hysteresis loop of the wire was measured during annealing using an AC current superposed upon a DC current. At the Curie temperature, the wire lost its ferromagnetic properties and its hysteresis loop disappeared. The annealing characteristic of the wire,  $T_{\text{ann}}(I_{\text{DC}})$ , was determined from Newton's Law of cooling (see Fig. 5). This characteristic shows that the Curie temperature is reached at 140 mA. The change in slope which occurs at 150 mA is due to the wire structure changing from amorphous to crystalline.

The following procedure was used to induce a permanent biasing in melt-extracted wires:

1. Each wire was stressed at approximately 100 MPa;
2. Each wire was heated under stress using DC currents of 50, 75 or 100 mA;
3. The annealing temperature was  $62.5$ ,  $100$  or  $165^{\circ}$  C, respectively;
4. At each temperature, the annealing time was 5, 10, 15 or 20 minutes.

The GMI responses of several 4 cm long wires following step 1 of this procedure show that the positive peaks of the GMI responses, taken from positive to negative DC fields, are located at about 1 Oe, in conformity with Fig. 1. This situation changes significantly after steps 2 to 4: the peak fields of wires heated by 50 mA currents diminish to about 0.65 Oe, and the slope of the response is higher than that before stress-annealing. (This results in sensors with sensitivities higher than that of the stressed wire before annealing.) For an annealing current of 75 mA, the peak fields stay about the same (0.85 – 0.9 Oe). Finally, at an annealing current of 100 mA, the peak fields increase, ranging from 1.4 to 1.8 Oe, and the slope of the response is lower than that before stress-annealing. (Sensors with sensitivities lower than those of wires before annealing were obtained in the latter case).

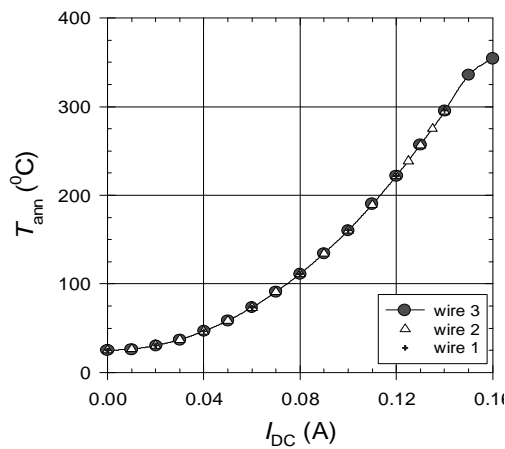


Fig. 5. Annealing temperature vs. annealing current for 35 – 40  $\mu\text{m}$  diameter melt-extracted wires.

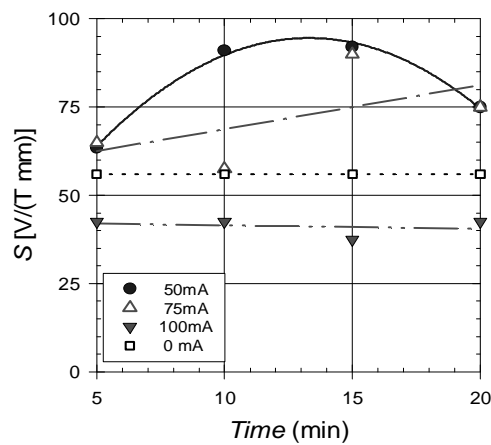


Fig. 6. Technical sensitivity vs annealing time for different DC annealing currents carried by the 4 cm long wires stressed at 100 MPa.

If these stress-annealed wires are used as sensing elements for GMI magnetic field sensors [11], the technical sensitivity of the sensor can be defined as the slope of its response around the field origin,  $\Sigma = \Delta U / (\Delta H \times l)$ , where  $\Delta U = \Delta Z \times I$ , and is expressed in Volts/(Tesla mm).  $\Delta Z$  is the range of the linear variation of the impedance with magnetic field,  $\Delta U$  is that of the output voltage,  $\Delta H$  is the linear magnetic field range,  $I$  is the amplitude of the driving current and  $l$  the length of the wire. The figure of merit of the sensor, defined as  $MF = (\Delta Z \times \Delta H) / l$  and expressed in  $\Omega \text{ T/mm}$ , takes into account the width of the linear magnetic field range detectable by the sensor. DC magnetic field biasing of the wire may be necessary if the linear segment of the GMI response is to intersect the zero field axis.

The variation of the technical sensitivity with annealing time is shown in Fig. 6 for 4 cm long wires under a tensile stress of 100 MPa. Before annealing, the wire sensitivity was about 55 V/(T mm).  $S$  shows a flat maximum with time of about 87.5 V/(T mm) following a 50 mA anneal for 10 – 15 min. The sensor sensitivity generally increases in this case. The sensitivity is around 75 V/(T mm) for a current of 75 mA, increasing slightly with the annealing time. For an annealing current of 100 mA, the sensitivity drops to about 37.5 V/(T mm) and decreases slightly with time. A stress higher than the applied stress is quenched in the wire following an annealing at high current. This results in obtaining a sensor with a technical sensitivity lower than that of the wire before annealing.

## 5. Conclusions

Current annealing of the wire was performed under a 100 MPa tensile stress. The optimum annealing time is about 15 minutes. The strength of the annealing current must be chosen so as to

quench-in the technical sensitivity needed for the sensor. We recommend 75 mA. The sensitivity can be further enhanced by increasing the amplitude of the sensing current while keeping the wire in a linear GMI regime. However, applications where power supply is critical must use the lowest current amplitude for which the giant magnetoimpedance in magnetic conductors continues to be a useful effect.

### References

- [1] F. B. Humphrey, K. Mohri, J. Yamasaki, H. Kawamura, R. Malmhall, I. Ogasawara, in A. Hernando, V. Madurga, M. C. Sanchez and M. Vazquez (eds), *Magnetic properties of amorphous metals*, North Holland, Amsterdam (1987) p. 110.
- [2] J. G. S. Duque, A. E. P. de Araujo, M. Knobel, A. Yelon, P. Ciureanu, *Appl. Phys. Lett.*, **83**, 99 (2003).
- [3] P. Ciureanu, I. Khalil, L. G. C. Melo, P. Rudkowski, A. Yelon, *J. Magn. Magn. Mater.*, **249**, 305 (2002).
- [4] K. Mohri, K. Kawashima, T. Kohzawa, H. Yoshida, *IEEE Trans. Magn.*, **29**, 1245 (1993).
- [5] P. Ciureanu, L. G. C. Melo, A. Yelon, *J. Magn. Magn. Mater.*, **242-245**, 224 (2002).
- [6] C. Gomez-Polo, M. Vazquez, *J. Magn. Magn. Mater.*, **118**, 86 (1993).
- [7] Y.-F. Li, M. Vazquez, D.-X. Chen, *J. Magn. Magn. Mater.*, **249**, 342 (2002).
- [8] D. Menard, D. Frankland, P. Ciureanu, A. Yelon, M. Rouabhi, R. W. Cochrane, H. Chiriac, T. A. Ovari, *J. Appl. Phys.*, **83**, 6566 (1998).
- [9] C. Gomez-Polo, M. Knobel, K. R. Pirotam, M. Vazquez, *Physica B*, **299**, 322 (2001).
- [10] L. Clime, G. Rudkowska, J. G. S. Duque, A. E. P. de Araujo, M. Knobel, P. Ciureanu, A. Yelon, *Physica B*, **343**, 410 (2003).
- [11] P. Ciureanu, P. Rudkowski, A. Yelon, U.S. Patent Application 2002/0135364, Sept. 26, 2002, allowed August 29, 2003.